

RSC Advances



This is an *Accepted Manuscript*, which has been through the Royal Society of Chemistry peer review process and has been accepted for publication.

Accepted Manuscripts are published online shortly after acceptance, before technical editing, formatting and proof reading. Using this free service, authors can make their results available to the community, in citable form, before we publish the edited article. This *Accepted Manuscript* will be replaced by the edited, formatted and paginated article as soon as this is available.

You can find more information about *Accepted Manuscripts* in the [Information for Authors](#).

Please note that technical editing may introduce minor changes to the text and/or graphics, which may alter content. The journal's standard [Terms & Conditions](#) and the [Ethical guidelines](#) still apply. In no event shall the Royal Society of Chemistry be held responsible for any errors or omissions in this *Accepted Manuscript* or any consequences arising from the use of any information it contains.

COMMUNICATION

A BODIPY-based fluorescent probe for the differential recognition of Hg(II) and Au(III) ions

Cite this: DOI: 10.1039/x0xx00000x

Ceren Cantürk, Muhammed Üçüncü and Mustafa Emrullahoğlu*

Received 00th January 2012,
Accepted 00th January 2012

DOI: 10.1039/x0xx00000x

www.rsc.org/

We describe the design, synthesis and spectral behaviour of a fluorescent molecular sensor able to recognize Hg²⁺ and Au³⁺ ions via different emission modes. The molecular sensor is constructed on a single BODIPY dye appended with semithiocarbazone functionality as a recognition motif.

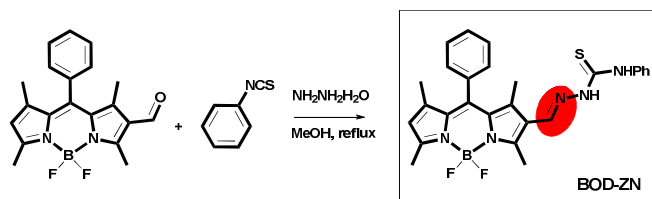
In recent years, research on the development of molecular sensors for analysing diverse biologically and environmentally important analyte species has increased.¹ While the vast majority of sensors addressed in such literature are designed to recognize a specific target, less common are sensors capable of differentiating multiple targets. Differential detection of multiple analyte species can be achieved best by recognizing each species through a different signal output (i.e., emission wavelength).² Incorporating multiple binding motifs onto a single signal-transducing molecule (chromophore/fluorophore) and, as an alternative, combining different transducing molecules have both appeared as efficient routes for sensors with multiple output modes.³

Despite recent advances in the field, it remains a challenge to differentiate metal species with similar chemical natures. For example, the ionic species of gold (Au³⁺) and mercury (Hg²⁺) share several similarities in terms of binding properties, since both have strong binding affinities toward sulphur species. When accumulated in the biological system, they thus have great potential to interact with sulphur-bearing biomolecules such as enzymes, proteins, and DNA. As a result, these metal species can disturb a series of cellular processes that cause toxicity in humans.^{3,4} Tracking these metal species in a living environment with the aid of a fluorescent molecular sensor is thus crucial to evaluating their roles in certain biological processes.

In their structure, most molecular sensors devised for mercury ions use sulphur moieties as a recognition motif.⁵ As such, it is always possible that gold and mercury species interfere with each other during their analysis, which could primarily explain why molecular sensors able to differentiate these two metal ions are extremely rare.⁶ Molecular tools that can differentiate multiple analytes of a similar chemical nature (e.g., gold⁷ and mercury^{5,8} ions) are therefore clearly in high demand.

Herein, we designed a molecular sensor with a single fluorophore core appended with semithiocarbazone functionality as the metal ion

recognition motif. The fluorophore core, based on a BODIPY dye,⁹ is designed to be inactive (i.e., non-emissive) in its initial state yet expected to become active in response to the metal species (Scheme 1). The differential detection of Hg²⁺ and Au³⁺ relies on different modulation mechanisms and can be realized with two distinct fluorescence changes, based on either an Hg²⁺-ligand coordination event or a gold-mediated chemical transformation.



Scheme 1 Synthesis of BOD-ZN.

The title compound, **BOD-ZN**, was prepared (40% overall) by the synthetic route outlined in Scheme 1 and, its structure was unambiguously confirmed by ¹H-NMR, ¹³C-NMR, and HRMS spectroscopy.¹⁰

The sensing behaviour of **BOD-ZN** toward the addition of a range of metal ion species was studied by UV/Vis and fluorescence spectroscopy. As shown in Figure 1a, the UV/Vis spectrum of free **BOD-ZN** (Phosphate buffer/Ethanol 1:4, pH 7.0) displays a maximum absorption band at 533 nm, which belongs to the BODIPY chromophore. The fluorescence spectrum of **BOD-ZN** collected upon excitation at 460 nm exhibits a very weak emission band at 601 nm. Reasonably, **BOD-ZN** was nearly non-emissive, since the molecular structure of the probe bears a C=N functionality that diminishes the emission of the BODIPY core caused by a non-radiative deactivation process involving the rapid isomerization of the C=N group.

Our investigation began with the evaluation of the optical behaviour of **BOD-ZN** in response to the addition of Au³⁺ ions (e.g., AuCl₃). The addition of Au³⁺ (1 equiv.) to **BOD-ZN** prompted the appearance of a new emission band at 512 nm that was assigned to the formation of a new BODIPY derivative (Fig. 1b). The appearance of this new band was accompanied with a distinct change in the solution's emission colour; the red-emitting probe solution

became distinctly green, as was clearly visible to the naked eye (Fig. S19, ESI†).

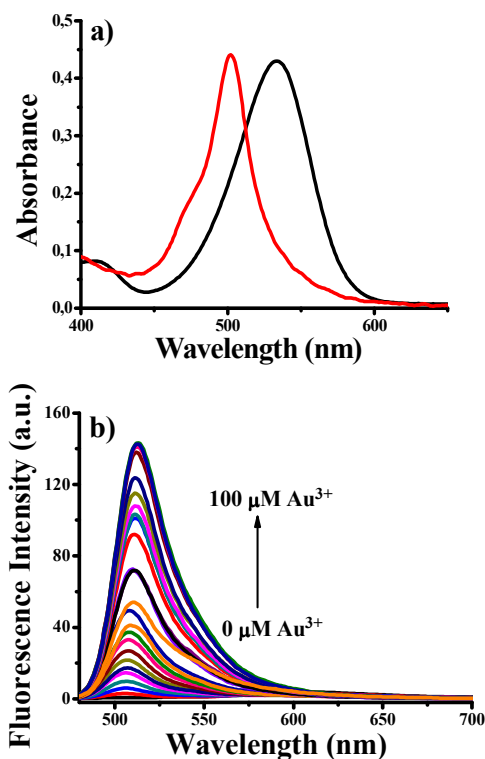
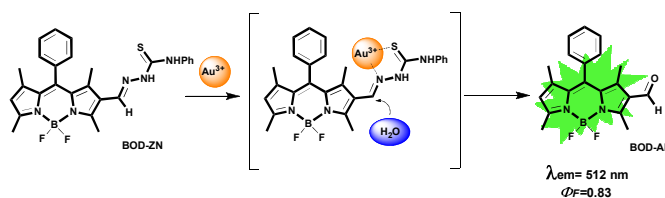


Fig. 1 (a) Absorbance spectra of **BOD-ZN** (10 μM) in the absence (black line) and presence (red line) of 10 equiv. (100 μM) of Au^{3+} ; (b) Fluorescence titration spectra of **BOD-ZN** (10 μM) + Au^{3+} (0.1 to 100 μM , 0.01 to 10 equiv.) in 0.1 M phosphate buffer / EtOH (pH 7.0, v/v, 1:4) (25°C, $\lambda_{\text{ex}}=460$ nm).

The compound displaying such green emission was isolated and further characterized as **BOD-AL**, the hydrolysis product of **BOD-ZN** (Scheme 2). Evidently, the recognition of Au^{3+} was based on an Au^{3+} -mediated hydrolysis reaction that resulted in the formation of a highly emissive BODIPY derivative (**BOD-AL**).

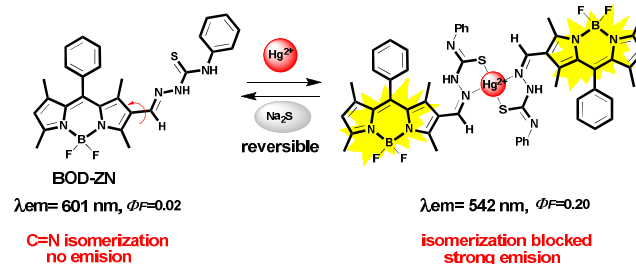


Scheme 2 Hydrolysis mechanism of **BOD-ZN** in the presence of Au^{3+} ions.

A systematic titration of **BOD-ZN** with Au^{3+} reveals that emission band intensity increases linearly with the increase in concentration of Au^{3+} in the range of 0.1–100 μM (Fig. S6, ESI†). At the same time, the kinetic study showed that the spectral response toward the addition of Au^{3+} was rapid (<1 min) and that the emission intensity plateaued within 20 min. due to the addition of 10 equiv. of Au^{3+} , which thereby enhanced intensity by over 200-fold. Moreover, the minimum amount of Au^{3+} detectable was evaluated to be 128.0 nM based on the signal-to-noise ratio (S/N=3) (Fig. S2, ESI†). Having established that the detection of Au^{3+} ions relies on an irreversible chemical reaction, we investigated the selectivity profile

of **BOD-ZN** in response to other metal species. The probe proved to be highly specific for Au^{3+} ions, since no change was detected in the spectrum when Au^{3+} ions were present. Furthermore, **BOD-ZN** showed no spectral response to other metal ions such as Cu^{2+} , Ag^{+} , Zn^{2+} , Pb^{2+} , Ni^{2+} , Na^{+} , Mg^{2+} , Li^{+} , K^{+} , Pd^{2+} , Fe^{3+} , Co^{2+} , Cd^{2+} , Ca^{2+} , Ba^{2+} , Fe^{3+} , and Cr^{3+} , except for Hg^{2+} .

We recognized the detection of Hg^{2+} with a different emission output. Given the addition of Hg^{2+} , the weakly emissive probe solution immediately (<5 sec) turned profoundly yellow, possibly due to the blockage of the C=N isomerization via strong coordination to the nitrogen electron pair which prevents the electron transfer process, and thus enhances the fluorescence emission (Scheme 3).



Scheme 3 Reversible binding of Hg^{2+} to **BOD-ZN**.

Meanwhile, in the fluorescence spectrum of **BOD-ZN**, a new emission band appeared at 542 nm and increased linearly with the increased concentration of Hg^{2+} above the range of 0.1–100 μM (Fig. 2b). The detection limit of **BOD-ZN** for detecting Hg^{2+} was 160.0 nM.

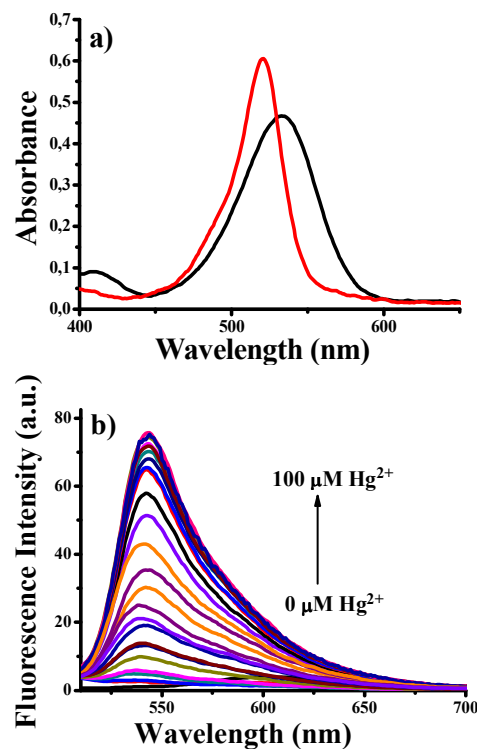


Fig. 2 (a) Absorbance spectra of **BOD-ZN** (10 μM) in the absence (black line) and presence (red line) of 10 equiv. (100 μM) of Hg^{2+} ; (b) Fluorescence titration spectra of **BOD-ZN** (10 μM) + Hg^{2+} (0.1

to 100 μM , 0.01 to 10 equiv.) in 0.1 M phosphate buffer / EtOH (pH 7.0, v/v, 1:4) (25°C, $\lambda_{\text{ex}}=460$ nm).

In sharp contrast to the detection of Au^{3+} , detecting Hg^{2+} ions proceeded reversibly. The reversibility of the binding event between **BOD-ZN** and Hg^{2+} was confirmed by the addition of Na_2S to the solution pre-treated with Hg^{2+} , which sharply decreased the emission intensity. The regeneration of fluorescence was again made possible by introducing Hg^{2+} ions into the solution, and the off-on switching ability of the system with Hg^{2+} proved the reversibility of the process (Fig. S15, ESI†).

At the same time, the binding process of Hg^{2+} to **BOD-ZN** could be clearly followed by the aid of $^1\text{H-NMR}$ spectroscopy. During Hg^{2+} incubation lasting 5 min, we observed pronounced differences in the $^1\text{H-NMR}$ spectrum of **BOD-ZN**. For one, the resonance of the H_a proton signal at 8.01 ppm belonging to the hydrogen atom of the aldimine shifted to a higher frequency, while the resonance of the methyl protons (H_b and H_c) in close proximity to the recognition motif shifted to a lower frequency. Furthermore, a reorganization of the phenyl ring proton signals strongly suggests the structural modification in the phenyl thiourea motif.

The stoichiometry of the sensing event was established by following the Benesi-Hildebrand method and, accordingly, the related binding constant was determined as $4.2 \times 10^4 \text{ M}^{-2}$.¹¹ With HRMS analysis, we also confirmed the binding of Hg^{2+} ions to **BOD-ZN**. HRMS data of the solution ($\text{Hg}^{2+}/\text{BOD-ZN}$) indicated the formation of an Hg^{2+} ion complex, ($m/z = 1204.36841$ found; 1204.36354 calc.), with a binding stoichiometry of 1:2.¹⁰ Given all of the above, the structure of the binding complex is most likely that shown in Scheme 3.

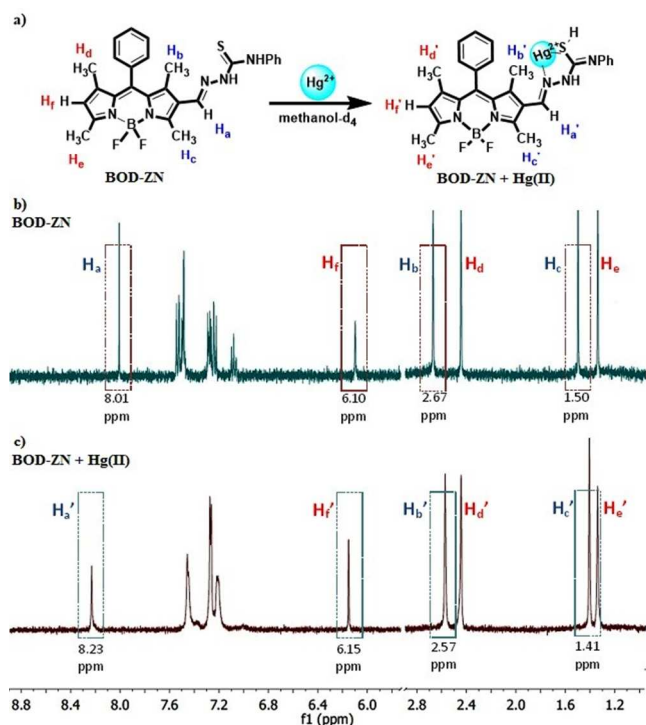


Fig. 3 (a) Proposed coordination mechanism of Hg^{2+} to **BOD-ZN**; (b) $^1\text{H-NMR}$ of **BOD-ZN** in methanol- d_4 ; (c) $^1\text{H-NMR}$ of **BOD-ZN** + Hg^{2+} (1 equiv.) in methanol- d_4 .

Having clarified the detection of both metal species, we assessed the interference of other metal ions in the detection of Au^{3+} and Hg^{2+} . Although the spectral response of **BOD-ZN** induced by Au^{3+} ions

showed no interference with other metal ions, the detection of Hg^{2+} was disturbed in the presence of Au^{3+} ions. More specifically, in the presence of Au^{3+} and Hg^{2+} , the fluorescence spectrum initially displayed an emission band at 542 nm for the $\text{Hg}^{2+}/\text{BOD-ZN}$ binding complex. However, the band disappeared within 10 min, as a new band appeared at 512 nm, which indicates that Au^{3+} ions also mediate the hydrolysis of the Hg^{2+} binding complex (Fig. S18, ESI†). Notably, the same sensing behaviour was also observed by adding Au^{3+} ions to a solution pre-treated with Hg^{2+} .

Relying on the impressive sensing properties of **BOD-ZN**, we next investigated its capacity for imaging Hg^{2+} and Au^{3+} ions in living cells. As Fig. 4a and 4a' show, the images of human lung adenocarcinoma (A549) cells incubated with **BOD-ZN** did not display any fluorescence until the addition of the metal species. However, upon incubation with Au^{3+} or Hg^{2+} , the cells started to emit a distinct fluorescence emission consistent with results obtained in the solution. Based on the nucleus staining experiment using DAPI as the staining dye, we concluded that the probe passes through the cell membrane and detects both metal species from within the cell. This preliminary cell imaging study suggested that **BOD-ZN** can be used efficiently for the in vitro imaging of Au^{3+} and Hg^{2+} species in living cells.

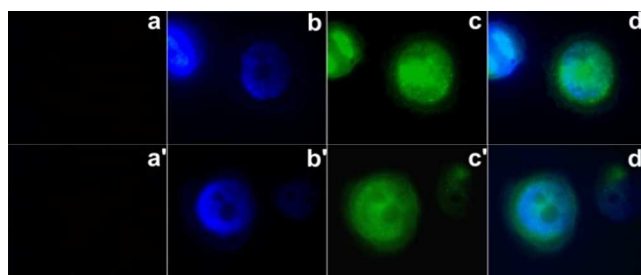


Fig. 4 Fluorescence images of Human Lung Adenocarcinoma cells (A549). (a, a') Fluorescence image of A549 cells treated with only **BOD-ZN** (10 μM); (b, b') Fluorescence image of cells treated with DAPI (control); (c, c') Fluorescence image of cells treated with **BOD-ZN** (10 μM) and Au^{3+} (10 μM) or Hg^{2+} (10 μM) ($\lambda_{\text{ex}} = 460$ nm); (d, d') merged images of frames b-c or b'-c'.

Conclusions

To close, we have studied the design, spectral behaviour, and cell-imaging capacity of a unique fluorescent molecular structure that can efficiently differentiate Hg^{2+} and Au^{3+} ions. The differential detection of Hg^{2+} and Au^{3+} was recognized in two distinct fluorescence changes: one resulting from a reversible Hg^{2+} /sensor complex formation, the other an irreversible Au^{3+} -mediated hydrolysis reaction. This novel molecular structure displayed the ability to recognize both metal species at nanomolar levels.

Notes and references

^a Department of Chemistry, Faculty of Science, İzmir Institute of Technology, Urla, 35430, İzmir, Turkey. E-mail: mustafaemrullahoglu@iyte.edu.tr..

† Electronic Supplementary Information (ESI) available: Absorbance, fluorescence and characterization data and all experimental procedures.. See DOI: 10.1039/c000000x/

1 For recent reviews, see: (a) M. E. Jun, B. Roy and K. H. Ahn, *Chem. Commun.*, 2011, **47**, 7583-7601; (b) H. Zheng, X.-Q. Zhan, Q.-N.

- Bian and X.-J. Zhang, *Chem. Commun.*, 2013, **49**, 429-447; (c) X. Chen, T. Pradhan, F. Wang, J. S. Kim and J. Yoon, *Chem. Rev.*, 2012, **112**, 1910-1956; (d) K. P. Carter, A. M. Young and A. E. Palmer, *Chem. Rev.*, 2014, **114**, 4564-4601; (e) X. Li, X. Gao, W. Shi and H. Ma, *Chem. Rev.*, 2014, **114**, 590-659.
- 2 (a) L. Xue, Q. Liu and H. Jiang, *Org. Lett.*, 2009, **11**, 3454-3457; (b) V. Luxami, Renukamal, K. Paul and S. Kumar, *RSC Adv.*, 2013, **3**, 9189-9192; (c) H. Komatsu, T. Miki, D. Citterio, T. Kubota, Y. Shindo, Y. Kitamura, K. Oka and K. Suzuki, *J. Am. Chem. Soc.*, 2005, **127**, 10798-10799; (d) M. Yuan, W. Zhou, X. Liu, M. Zhu, J. Li, X. Yin, H. Zheng, Z. Zuo, C. Ouyang, H. Liu, Y. Li and D. Zhu, *J. Org. Chem.*, 2008, **73**, 5008-5014; (e) D. Maity and T. Govindaraju, *Chem. Commun.*, 2012, **48**, 1039-1041; (f) P. N. Basa and A. G. Sykes, *J. Org. Chem.*, 2012, **77**, 8428-8434; (g) L. Cao, J. Cia, Y. Huang, Q. Zhang, N. Wang, Y. Xue and D. Du, *Tetrahedron Lett.*, 2014, **55**, 4062-4066; (h) N. R. Chereddy, P. Nagaraju, M. V. Niladri Raju, K. Saranraj, S. Thennarasu and V. J. Rao, *Dyes Pigm.*, 2015, **112**, 201-209; (i) L. Fan, J.-C. Qin, T.-R. Li, B.-D. Wang and Z.-Y. Yang, *Sens. Actuators, B*, 2014, **203**, 550-556.
- 3 I. Onyido, A. R. Norris and E. Buncl, *Chem. Rev.*, 2004, **104**, 5911-5929.
- 4 E. Nyarko, T. Hara, D. J. Grab, A. Habib, Y. Kim, O. Nikolskaia, T. Fukuma and M. Tabata, *Chem.-Biol. Interact.*, 2004, **148**, 19-25.
- 5 (a) Y.-K. Yang and K.-J. Yook, *J. Am. Chem. Soc.*, 2005, **127**, 16760-16761; (b) J.-S. Wu, I.-C. Hwang, K. S. Kim and J. S. Kim, *Org. Lett.*, 2007, **9**, 907-910; (c) G.-Q. Shang, X. Gao, M.-X. Chen, H. Zheng and J.-G. Xu, *J. Fluoresc.*, 2008, **18**, 1187-1192; (d) S. Atilgan, T. Ozdemir and E.U. Akkaya, *Org. Lett.*, 2010, **12**, 4792-4795; (e) Q. Zhang, X.-J. Huang and Z.-J. Zhu, *RSC Adv.*, 2013, **3**, 24891-24895; (f) S. Chen, P. Wang, C. Jia, Q. Lin and W. Yuan, *Spectrochim. Acta, Part A*, 2014, **133**, 223-228; (g) H. N. Kim, S.-W. Nam, K. M. K. Swamy, Y. Jin, X. Chen, Y. Kim, S.-J. Kim, S. Park and J. Yoon, *Analyst*, 2011, **136**, 1339-1343.
- 6 (a) M. Dong, Y.-W. Wang and Y. Peng, *Org. Lett.*, 2010, **12**, 5310-5313; (b) E. Karakuş, M. Üçüncü and M. Emrulloğlu, *Chem. Commun.*, 2014, **50**, 1119-1121.
- 7 (a) M. J. Jou, X. Chen, K. M. K. Swamy, H. N. Kim, H. -J. Kim, S. G. Lee and J. Yoon, *Chem. Commun.*, 2009, 7218-7220; (b) O. A. Egorova, H. Seo, A. Chatterjee and K. H. Ahn, *Org. Lett.*, 2010, **12**, 401-403; (c) Y. K. Yang, S. Lee and J. Tae, *Org. Lett.*, 2009, **11**, 5610-5613; (d) J. Y. Choi, G. -H. Kim, Z. Guo, H. Y. Lee, K. M. K. Swamy, J. Pai, S. Shin, I. Shin and J. Yoon, *Biosens. Bioelectron.*, 2013, **49**, 438-441; (e) J. -B. Wang, Q. -Q. Wu, Y. -Z. Min, Y. -Z. Liu and Q. -H. Song, *Chem. Commun.*, 2012, **48**, 744-746; (f) M. Üçüncü and M. Emrulloğlu, *Chem. Commun.*, 2014, **50**, 5884-5886; (g) H. Seo, M. E. Jun, O. A. Egorova, K. H. Lee, K. T. Kim and K. H. Ahn, *Org. Lett.*, 2012, **14**, 5062-5065; (h) M. Emrulloğlu, E. Karakuş and M. Üçüncü, *Analyst*, 2013, **138**, 3638-3641.
- 8 For recent reviews, see: (a) M. J. Culzoni, A. Muñoz de la Peña, A. Machuca, H. C. Goicoechea and R. Babiano, *Anal. Methods*, 2013, **5**, 30-49; (b) Z. Yan, M. -F. Yuen, L. Hu, P. Sun and C. -S. Lee, *RSC Adv.*, 2014, **4**, 48373-48388; (c) P. Mahato, S. Saha, P. Das, H. Agarwalla and A. Das, *RSC Adv.*, 2014, **4**, 36140-36174.
- 9 For recent reviews, see: (a) N. Boens, V. Leen and W. Dehaen, *Chem. Soc. Rev.*, 2012, **41**, 1130-1172; (b) R. Ziessel, G. Ulrich and A. Harriman, *New J. Chem.*, 2007, **31**, 496-501; (c) A. Loudet and K. Burgess, *Chem. Rev.*, 2007, **107**, 4891-4932; (d) G. Ulrich, R. Ziessel and A. Harriman, *Angew. Chem., Int. Ed.*, 2008, **47**, 1184-1201.
- 10 See the ESI† for more details
- 11 (a) H. A. Benesi, J. H. Hildebrand, *J. Am. Chem. Soc.* 1949, **71**, 2703-2707; (b) J. Hatai, S. Pal, G. P. Jose, T. Sengupta, S. Bandyopadhyay, *Rsc Adv.* 2012, **2**, 7033-7036.